Properties of single voltage-dependent K^+ channels in dendrites of CA1 pyramidal neurones of rat hippocampus

Xixi Chen and Daniel Johnston

Department of Neuroscience, Baylor College of Medicine, Houston, TX 77030, USA

Voltage-dependent K^+ channels in the apical dendrites of CA1 pyramidal neurones play important roles in regulating dendritic excitability, synaptic integration, and synaptic plasticity. Using cell-attached, voltage-clamp recordings, we found a large variability in the waveforms of macroscopic K^+ currents in the dendrites. With single-channel analysis, however, we were able to identify four types of voltage-dependent K^+ channels and we categorized them as belonging to delayed-rectifier, M-, D-, or A-type K^+ channels previously described from whole-cell recordings. Delayed-rectifier-type K^+ channels had a single-channel conductance of 19 ± 0.5 pS, and made up the majority of the sustained K^+ current uniformly distributed along the apical dendrites. The M-type K^+ channels had a single-channel conductance of 11 ± 0.8 pS, did not inactivate with prolonged membrane depolarization, deactivated with slow kinetics (time constant 100 ± 6 ms at −40 mV), and were inhibited by bath-applied muscarinic agonist carbachol (10 μM). The D-type K^+ channels had a single-channel conductance of around 18 pS, and inactivated with a time constant of 98 ± 4 ms at +54 mV. The A-type K^+ channels had a single-channel conductance of 6 ± 0.6 pS, inactivated with a time constant of 23 ± 2 ms at +54 mV, and contributed to the majority of the transient K^+ current previously described. These results suggest both functional and molecular complexity for K^+ channels in dendrites of CA1 pyramidal neurones.

(Resubmitted 13 May 2004; accepted after revision 23 June 2004; first published online 24 June 2004)
Corresponding author X. Chen: Department of Neuroscience, Baylor College of Medicine, Houston, TX 77030, USA.
Email: xixi@ltp.neusc.bcm.tmc.edu

Most excitatory and inhibitory inputs to hippocampal CA1 pyramidal neurones form synapses on the dendrites (Megias *et al.* 2001). The electrical properties of the dendrites largely determine how synaptic potentials integrate and propagate to the soma. On the other hand, action potentials initiated in the soma/axon region of the cell back-propagate into the dendrites, the efficacy of which is also dependent on dendritic membrane properties (Johnston *et al.* 1996; Hausser *et al.* 2000). Direct patch-clamp recordings from the apical dendrites of CA1 pyramidal neurones have revealed the existence of a variety of ion channels, testifying to the active properties of the dendrites (Magee & Johnston, 1995; Hoffman *et al.* 1997; Magee, 1998; Mickus *et al.* 1999). Most remarkably, recordings of macroscopic K^+ currents led to the discovery of a non-uniform distribution of the fast inactivating A-type K^+ currents along the dendrites, with the distal dendrite having an average density of A-current that is approximately five times the average density of A-current in the soma (Hoffman *et al.* 1997).

In CA1 pyramidal neurones, several types of K^+ currents have been described with whole-cell, voltage-clamp recordings. Each of them contributes to the cell's firing behaviour in a unique way (Storm, 1990). At least four types of such currents are solely voltage dependent. The A-type K^+ current has the most rapid inactivation kinetics, the D-type K^+ current has slower inactivation, while the delayed-rectifier K^+ current inactivates much more slowly. Because of very slow inactivation kinetics, the delayed-rectifier K^+ current does not appear to inactivate during voltage steps of several hundred milliseconds. The M-type K^+ current, on the other hand, is a true non-inactivating current that can be distinguished from other types of voltage-dependent K^+ currents by being active during prolonged membrane depolarization.

From cell-attached recordings of macroscopic K^+ currents, we know that fast inactivating A-currents and non-inactivating (for several hundred milliseconds) sustained currents are both found in the dendrites of

 DOI: 10.1113/jphysiol.2004.068114

CA1 pyramidal neurones. Compared to the A-current, the amplitude of the macroscopic sustained currents remains relatively small and constant along the dendrites (Hoffman *et al.* 1997). The identities of the channels contributing to these macroscopic currents are not known. Pharmacological agents that presumably block the D-type K^+ currents were also found to have significant effects on dendritic signalling (Golding *et al.* 1999; Bekkers & Delaney, 2001). Yet direct biophysical evidence for the dendritic presence of these channels has been scarce.

The cell-attached configuration of patch-clamp recording provides a patch-by-patch measurement of membrane currents along the dendrites, while preserving the intracellular milieu of the neurone. Macroscopic K^+ currents recorded in the cell-attached configuration displayed large variability in their waveforms, probably because each recording sampled only a subpopulation of the total current that is composed of different types of voltage-dependent K^+ channels. In a subset of our recordings, single K^+ channels could be resolved. With single-channel analysis, we found multiple types of K^+ channels each having a unique combination of biophysical properties.

Methods

Slice preparation

Acute hippocampal slices (400 μm thick) were prepared from 6- to 8-week-old Sprague-Dawley rats. Experiments were performed in accordance with Baylor and US governmental regulations of animal welfare. Animals were anaesthetized with a lethal dose of a combination of ketamine and xylazine (I.P.), perfused through the heart with ice-cold (4°C) cutting solution (described below), and decapitated. The brain was then dissected out and sliced using a Vibratome. The slices were transferred to a submerged holding chamber containing oxygenated external solution (described below). Pyramidal neurones of the hippocampal CA1 region were visualized with an Olympus 60× water immersion objective and a Zeiss Axioskop with infrared differential interference contrast (DIC). The apical dendrites of CA1 pyramidal neurones could be visually identified and followed for > 300 μm from the soma. All channel recordings were done at room temperature (22−24°C) for better resolution of single-channel events and better stability of the patch membrane.

Solutions and drugs

The solution used for animal perfusion and slicing contained (mM): 220 sucrose, 2.5 KCl, 1.25 NaH_2PO_4, 25 $NaHCO_3$, 0.5 $CaCl_2$, 7 $MgCl_2$, and 7 dextrose. During experiments, the slices were continuously superfused with oxygenated external solution containing (mM): 125 NaCl, 2.5 KCl, 1.25 NaH_2PO_4, 25 $NaHCO_3$, 2 $CaCl_2$, 1 $MgCl_2$, and 25 dextrose (pH 7.4 when saturated with 95% O_2 and 5% CO_2). For recordings of voltage-dependent K^+ channels, the pipette solution contained (mM): 125 NaCl, 2.5 KCl, 2 $CaCl_2$ (unless otherwise noted), 1 $MgCl_2$, 10 Hepes, and 1 μM TTX to block Na^+ channels (pH 7.4 with NaOH). TTX was stored in 2 mM aliquots and diluted to the desired concentration for experiments. During experiments where carbamylcholine chloride (carbachol) was bath-applied, the external solution also contained 1 μM TTX, 200 μM $CdCl_2$ and 100 μM $NiCl_2$ to prevent drastic changes of membrane potential and bursting of pyramidal cells. TTX was purchased from Alomone Laboratories (Jerusalem, Israel). All other reagents were purchased from Sigma (St Louis, MO, USA).

Data acquisition and analysis

Cell-attached recordings were made from the soma and apical dendrites of visually identified CA1 pyramidal neurones. Recording electrodes were pulled from thick-wall borosilicate glass pipettes (Sutter Instruments), either coated with Sylgard or wrapped with thin strips of parafilm (Mitterdorfer & Bean, 2002), and fire polished. The tips of the electrodes had similar diameters of $\sim$1 μm, with resistances of 5–7 MΩ when filled with the pipette solutions described above. Positive pressure was applied to the patch electrode while approaching dendrites in the slice. Tight seals of > 10 GΩ can be formed when releasing the pressure. Zero or minimum suction was applied. To measure the liquid junction potentials between the solutions, an agar bridge was made with 3 M KCl, which connected two baths. One of the baths was in contact with the electrode, the other was connected to the earth of the amplifier. The amplifier was first zeroed with the electrode and the two baths containing the same solution. Then the solution was changed in the bath in contact with the electrode, and the liquid junction potential was read from the amplifier. The liquid junction potential between the external solution and the NaCl-based pipette solution was < 1 mV (with reference to the electrode). After cell-attached recordings, the membrane patch was ruptured and the resting membrane potential of the cell (-66 ± 0.4 mV, $n = 135$) was recorded immediately after break-in. This potential was then used to calculate the absolute voltage of the commands. Liquid junction potential was not corrected for.

Recordings were performed using an Axopatch-1D voltage-clamp amplifier (Axon Instruments, Union City, CA, USA), and an ITC-18 computer interface (Instrutech, Port Washington, NY, USA). Data acquisition was controlled by custom software written in Igor

(WaveMetrics, Lake Oswego, OR, USA). Channel records were analog filtered at 2 kHz, digitized at 10 kHz, and digitally filtered at 1 kHz. Linear leak and capacitive currents were digitally subtracted using appropriately scaled null traces. For single-channel analysis, event detection was performed running custom-built Hidden Markov Models (HMM) incorporated in the TAC software (Bruxton, Seattle, WA, USA). The number of channels present in a patch was determined by counting the number of current levels at voltages where the open probability of the channel(s) was relatively high. Event tables and amplitude histograms were then exported from TAC as text files. Subsequent analyses of channel conductances and open probabilities were performed using custom software written in Igor. Single-channel conductance (γ) was calculated as the slope of the best line fit to the single-channel current–voltage (i–V) scatter plot:

$$i = \gamma(V - V_{reversal})$$

The open probability of a channel was calculated as:

$$P_{\text{open}} = t_{\text{open}}/t_{\text{total}}$$

where t_{open} is the length of time that the channel was in the open state and t_{total} is the total time during the appropriate voltage command.

Activation and inactivation curves were fitted with single Boltzmann equations:

$$y = 1/\{1 + \exp[(V_{1/2} - V)/k]\}\ \text{(activation)}$$

$$y = 1 - 1/\{1 + \exp[(V_{1/2} - V)/k]\}\ \text{(inactivation)}$$

$V_{1/2}$ is the voltage for half-maximum activation (inactivation), and k is the slope of the curve.

Analyses of channel open/closed durations were performed using TACFit (Bruxton). Events of < 1 ms duration were excluded from analyses. Logarithmic duration histograms of open and closed times were fitted with exponential distribution functions:

$$f(t) = \Sigma[(\text{weight}_i/\tau_i)\exp(-t/\tau_i)]$$

Where appropriate, data are expressed as mean ± standard error of the mean (S.E.M.). Student's t test was used to determine whether the difference between pairs of treatment groups was statistically significant ($P < 0.05$).

Results

Variability in the waveform of macroscopic K^+ currents as recorded from the dendrites of CA1 pyramidal neurones in the cell-attached configuration

A total of 215 cell-attached recordings were made from both the soma ($n = 49$) and the apical dendrites ($n = 166$, 50–330 μm from soma) of CA1 pyramidal neurones, using pipette solutions that mimic the ion composition of the external solution (NaCl-based, see Methods). The membrane was held at −30 mV relative to rest (typically around −96 mV when the cell's resting membrane potential was corrected for, see Methods), and stepped to depolarized potentials of up to +120 mV relative to rest (typically around +54 mV after correcting for the cell's resting membrane potential). K^+ currents were identified by their outward polarity.

In Fig. 1, 17 examples of ensemble averaged K^+ currents (activated by 400 ms voltage steps from approximately −96 mV to +54 mV) are presented. These recordings were from different CA1 pyramidal neurones but at a similar location in the apical dendrites (220 ± 3 μm from soma, $n = 17$). The waveforms of the ensemble averaged K^+ currents, reflecting time-dependent inactivation kinetics, are highly variable. This observation suggests that there are different types of K^+ channels in the dendrites with different time-dependent inactivation kinetics, and that each cell-attached recording sampled a different combination of these channels.

In a subset of our cell-attached recordings ($n = 32$; 5 somatic recordings, 27 dendritic recordings 50–300 μm from soma), the activities of single K^+ channels could be resolved. By performing detailed single-channel analyses on these records, we could identify different types of single K^+ channels with distinct time-dependent inactivation kinetics.

The accuracy of single-channel analyses declines with increasing numbers of channels present in a patch. Single-channel analyses of channel biophysics were therefore performed only when the recorded patch had 1–3 channels of the same conductance ($n = 26$), or 2 channels of different conductances ($n = 6$). The rest of the recordings (183 out of 215) were of macroscopic K^+ currents where it was hard to tell apart the underlying single channels, especially at very depolarized voltages. Some of these recordings were included in the analysis of time-dependent inactivation/deactivation kinetics or channel pharmacology, only when certain types of currents (for example the D-type, $n = 4$) or channels (for example the M-type, $n = 5$) could be unambiguously identified with certain voltage protocols (see below, Table 1).

Delayed-rectifier K^+ channels

Figure 2 illustrates a typical recording at 200 μm from the soma, with only one delayed-rectifier K^+ channel in the patch. During depolarizing voltage steps of −18 mV (from a holding potential of −98 mV), discrete channel opening events started to appear. As the membrane was stepped to more and more depolarized potentials, the channel spent increasingly more time in the open state and less time in the closed state (Fig. 2*A*). In this particular

example there was only one channel, which probably had one amplitude state; therefore the amplitude histograms had two peaks (Fig. 2*B*). The first (counting from the left) peak represents the current level when the channel was closed; the second peak represents the current level when the channel was open. The distance between these two peaks, as a rough measure of single-channel current amplitude, increased with membrane depolarization. This is because of a greater driving force for K^+ as the membrane was depolarized beyond the reversal potential of K^+ (-104 mV as calculated from the Nernst equation, and assuming 155 mM K^+ inside the cell; Fricker *et al.* 1999). Along with depolarization, there was also a change in the relative proportion of the two peaks in the histograms, with more events being in the open state (second peak) and concurrently fewer events in the closed state (first peak) (Fig. 2*B*). During voltage steps of up to 1 s, there was barely any time-dependent inactivation of the channel (Fig. 2*A*, bottom trace).

Plotting single-channel current amplitude against membrane voltage led to an amplitude scatter graph (Fig. 2*C*). At voltage levels between -20 mV and $+20$ mV, the *i–V* relation of this channel appeared to be linear. The slope of the line fit, as is shown in Fig. 2*C*, is an estimate of the single-channel conductance, which was 18 pS in this particular case.

When the open probability of the channel was plotted against membrane voltage, the voltage dependence of its activation became more obvious. Fitting the data with a Boltzmann equation resulted in an estimation of the voltage at which the channel was in the open state for 50% of the time ($V_{1/2}$): $+5$ mV in this example. The slope of the activation curve was $k = 7$ (Fig. 2*D*).

Voltage-dependent activation of this channel was also evident in the duration histograms where the durations of every channel opening/closing event were collected and fitted with exponential equations (Fig. 2*E*). The exponential equations are the theoretical probability–density functions of duration distribution of single channels. When plotted as square-root *y*-axis against logarithmic *x*-axis, each exponential component becomes a distinct peak, with the *x*-axis value of the peak being the time constant of this component. The time constant of each exponential component also corresponds to the mean duration of the events within this component (Colquhoun & Sigworth, 1995). At the membrane voltages shown in Fig. 2*E*, both the closed-time duration distribution and the open-time duration distribution were best fitted with two exponential components, of which the second (longer duration) components consisted of actual measurements while the peaks of the first (shorter duration) components were usually deduced from the fitting. With membrane

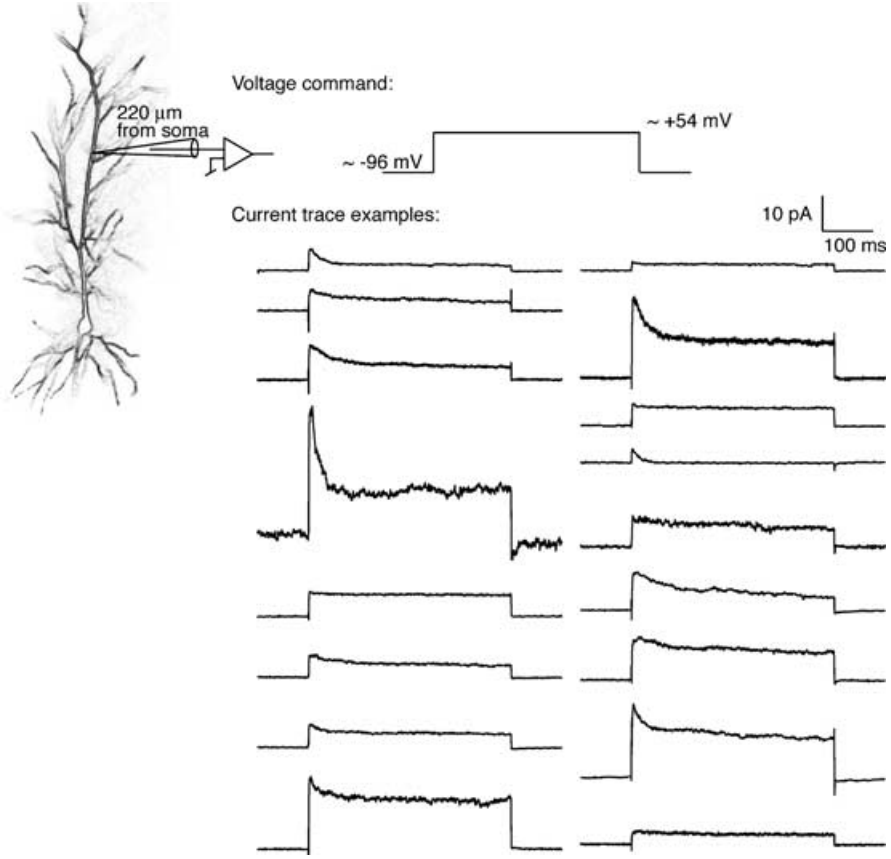

Figure 1. Variability of macroscopic K^+ currents
All current traces (ensemble averages of 3–20 sweeps) shown in this figure were recorded from dendritic patches at 220 ± 3 μm from soma. Electrodes used in these recordings had uniform diameters of ~ 1 μm. Minimum suction was applied during seal formation. K^+ currents were activated by a voltage step from approximately -96 mV to $+54$ mV, lasting 400 ms. Both the amplitude and the waveform of the macroscopic currents were highly variable.

Table 1. Summary of recordings

	Channel types	Total number of recordings	Number of somatic recordings	Number of dendritic recordings	Location of dendritic recordings (distance from soma in μm)
Recordings for single-channel analysis of channel biophysics	Delayed-rectifier K^+ channels	18	2	16	50–300
	M-type K^+ channels	7[a]	3	4	170–250
	D-type K^+ channels	1	0	1	240
	A-type K^+ channels	6	1	5	120–215
Additional recordings for analysis of inactivation/deactivation kinetics or channel pharmacology	Ensemble D-current	4	2	2	170, 240
	M-type K^+ channels	5	5	0	—

[a]Includes one recording where only one M-type channel was present in the patch, and six recordings where one delayed-rectifier channel and one M-type channel were coexisting in the same patch (these recordings were not included in the 18 recordings used for analysis of the delayed-rectifier channels).

depolarization, the mean open-time of the channel became longer while the mean closed-time of the channel became shorter (Fig. 2*E*).

From multiple recordings similar to the one shown in Fig. 2, the single-channel conductance of the delayed-rectifier type K^+ channels was calculated to be $\gamma = 19 \pm 0.5$ pS ($n = 16$) with a $V_{1/2}$ for activation of 2 ± 1 mV and $k = 7 \pm 0.4$ ($n = 15$), and a time constant for inactivation of 1.6 ± 0.3 s ($n = 9$) at approximately +50 mV (Table 2).

M-type K^+ channels

The difference between the delayed-rectifier K^+ channels and the M-type K^+ channels is best demonstrated in recordings where two such different channels were present in the same patch. Figure 3 illustrates such a recording at a dendritic location 230 μm from soma. At membrane voltages of around −30 mV (depolarized from a holding potential of −100 mV), channel openings of relatively small amplitude started to appear. With further depolarization, the delayed-rectifier K^+ channel in this patch was also activated (Fig. 3*A*). Single-channel conductances of the two channels in Fig. 3 were clearly different, giving rise to multiple peaks in the amplitude histograms (Fig. 3*B*). These peaks (counting from small-amplitude level to big-amplitude level) represent the current levels when both channels were closed; when the small-conductance channel alone was open; when the delayed-rectifier channel alone was open; and when both channels were open at the same time (Fig. 3*B*).

The delayed-rectifier K^+ channel in this recording had a single-channel conductance of 19 pS, $V_{1/2} = 9$ mV, and $k = 7.5$ for voltage-dependent activation. The smaller conductance channel, on the other hand, had a single-channel conductance of 10 pS in this recording (Fig. 3*C*), and $\gamma = 11 \pm 0.8$ pS for $n = 5$ such recordings where single-channel conductance could be reliably determined. It appears that the smaller conductance channel had a lower voltage threshold for activation, with significant channel activities measured at around −30 mV. Activation of the smaller conductance channel was voltage dependent, with $V_{1/2} = -6$ mV and $k = 17$ (Fig. 3*D*) ($V_{1/2} = -9 \pm 2$ mV, $n = 3$; $k = 20 \pm 2.2$, $n = 3$; Table 2). The smaller conductance channel, with its low voltage threshold for activation, was tentatively categorized as an M-type K^+ channel.

Duration analysis was only reliably obtained for one putative M-type K^+ channel (the same one as shown in Fig. 3). Single-component exponential distribution functions were fitted to both closed and open time histograms, showing increasing mean open times and decreasing mean closed times along with membrane depolarization (Fig. 4).

Time-dependent inactivation of the putative M-type K^+ channels was drastically different from that of the delayed-rectifier K^+ channels. Figure 5*A* shows two independent recordings, one being a delayed-rectifier K^+ channel (210 μm from soma), the other being a putative M-type K^+ channel (230 μm from soma). Both recordings were from prolonged membrane depolarization to +20 mV (from a holding potential of −70 mV) that lasted 15 s. The delayed-rectifier K^+ channel (upper trace), although seemingly 'non-inactivating' with voltage steps of up to 1 s, would eventually inactivate with depolarizations longer than 3 s. In contrast, the M-type K^+ channel (lower trace) did not inactivate even at the end of a 15 s depolarization. Being truly non-inactivating, this channel is well suited to account for the macroscopic M-type K^+ current.

The non-inactivating (for seconds) feature of the putative M-type K^+ channels served as a benchmark for us to separate these channels from other types of voltage-dependent K^+ channels. All one needed to do was to hold the membrane patch at a depolarized potential (+20 mV, for example) for longer than 10 s. Channel activities still remaining at the end of this 10 s depolarization should be

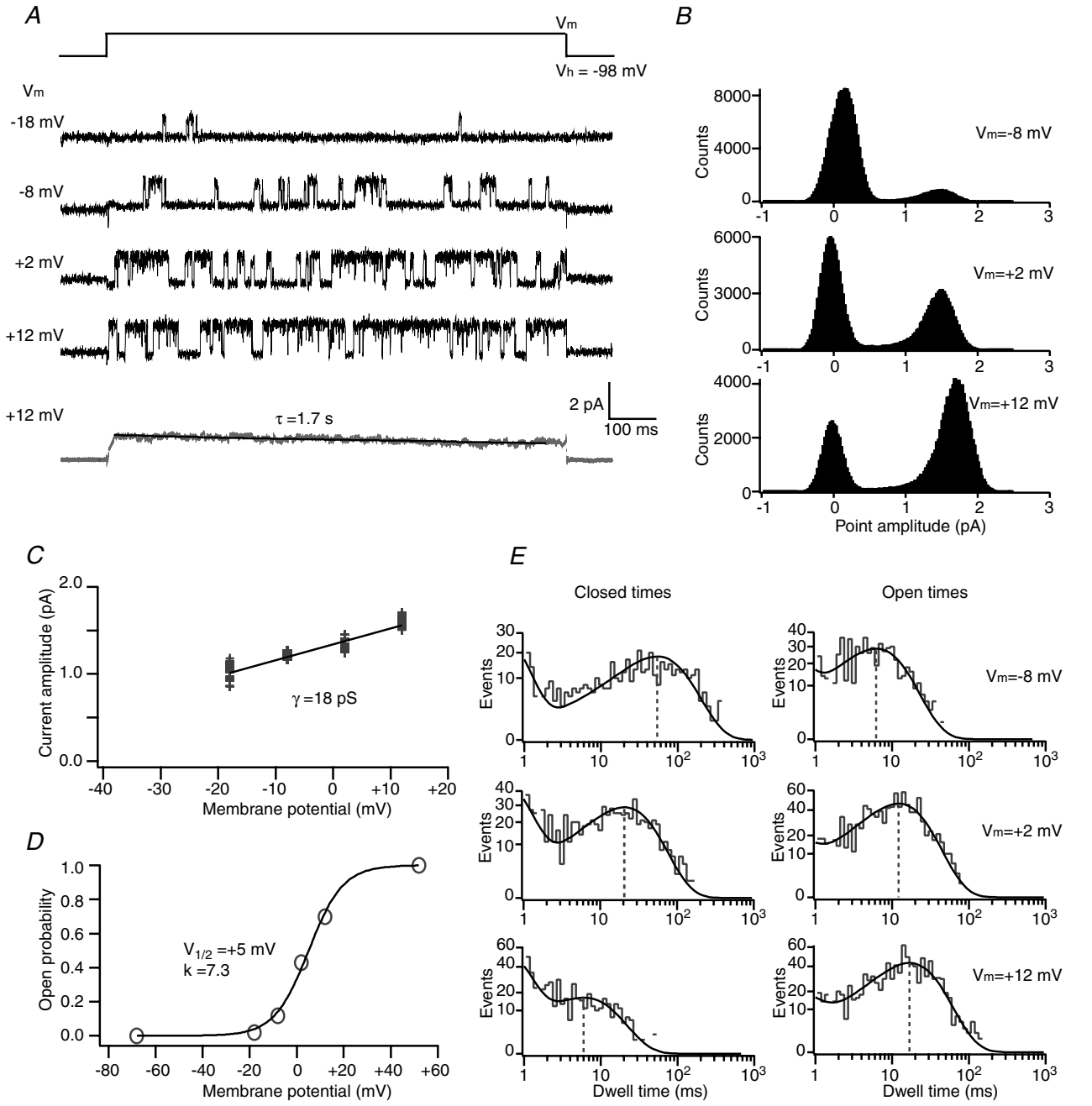

Figure 2. Single delayed-rectifier K^+ channel recorded 200 μm from soma
Only one delayed-rectifier-type K^+ channel was present in this recording. *A*, example traces of single-channel activity. The patch membrane was held at −98 mV. Voltage commands of 1000 ms were given to activate the channel. Channel activity increased with depolarization. Bottom trace is the ensemble average of recordings at +12 mV (average of 25 traces). Single exponential fitting to the ensemble average gave $\tau = 1.7$ s for time-dependent inactivation. *B*, current amplitude histograms of recordings at noted potentials. The left peak in each histogram represents current level when the channel was closed, while the right peak in the histogram represents current level when the channel was open. *C*, amplitude scatter graph. Current amplitude of the open state is plotted against command potential. The line fit to the amplitude scatter graph gave single-channel conductance (γ) of 18 pS. *D*, voltage-dependent activation. Open probability of the channel was plotted against command potential. Activation can be fitted with a single Boltzmann equation. In this particular recording, half-activation voltage ($V_{1/2}$) was +5 mV; slope of activation (k) was 7.3. *E*, duration analysis. Duration histograms were constructed for both closed and open times at noted potentials. The histograms could be best fitted with two-component exponential distribution functions (continuous lines). Dotted lines mark the time constants of the second components of each fit (τ_{c2} and τ_{o2}): $V_m = -8$ mV, $\tau_{c2} = 54$ ms, $\tau_{o2} = 6$ ms; $V_m = +2$ mV, $\tau_{c2} = 21$ ms, $\tau_{o2} = 12$ ms; $V_m = +12$ mV, $\tau_{c2} = 6$ ms, $\tau_{o2} = 17$ ms.

Table 2. Single-channel properties of dendritic K^+ channels

	Activation				Inactivation				Deactivation
	γ (pS)	Range (mV)	$V_{1/2}$ (mV)	k	Range (mV)	$V_{1/2}$ (mV)	k	τ [a]	τ [b] (ms)
Delayed-rectifier-type K^+ channel	19 ± 0.5 ($n = 16$)	-20 to $+50$	$+2 \pm 1$ ($n = 15$)	7 ± 0.4 ($n = 15$)				1.6 ± 0.3 s ($n = 9$)	
M-type K^+ channel [c]	11 ± 0.8 ($n = 5$)	< -30 to $+50$	-9 ± 2 ($n = 3$)	20 ± 2.2 ($n = 3$)					100 ± 6 ($n = 3$)
D-type K^+ channel	18 [d]	-20 to $+50$	$+4$	6	-50 to $+10$	-20	8	98 ± 4 ms ($n = 5$)	
A-type K^+ channel [e]	6 ± 0.6 ($n = 3$)	-60 to $+50$	$+5$	16	-80 to 0	-64	9	23 ± 2 ms ($n = 5$)	

γ, single-channel conductance. k, slope of Boltzmann equation. τ, time constant: [a] determined at $+50$ mV; [b] determined at -40 mV. [c] Determined with 0 Ca^{2+} in the recording pipette. [d] Mean of 3 channels in the same recording. [e] Voltage-dependent activation kinetics were determined by fitting normalized peak conductance averaged from 5 recordings; voltage-dependent inactivation kinetics were determined by fitting normalized peak current averaged from 3 recordings.

considered as coming from the putative M-type K^+ channels.

We next explored the deactivation kinetics of the putative M-type K^+ channels, because macroscopic M-current deactivates with characteristic slow kinetics. This slow deactivation, along with being truly non-inactivating, provides the basis for the 'classical' voltage protocol of recording macroscopic M-currents. Such a protocol normally involves holding the cell at a depolarized potential for a prolonged time, so that only M-currents remain active, and stepping to more negative potentials. With the M-current slowly deactivating, a seemingly inward current could be recorded, reflecting deactivation of an outward current (Brown & Adams, 1980; Adams *et al.* 1982). A similar protocol was applied in the somatic recording shown in Fig. 5*B* and *C*. To first isolate the putative M-type K^+ channels, we held the patch membrane at $+18$ mV for 10 s. Hyperpolarizing voltage steps to -12, -42 and -72 mV were applied afterwards to deactivate the channel(s) (Fig. 5*B*). At -12 mV, there were still appreciable channel activities so that the deactivation was not obvious. At -42 and -72 mV, the putative M-type K^+ channels deactivated with slow kinetics ($\tau = 99$ ms and 51 ms, respectively) to generate the relaxation current (Fig. 5*B*). After 1 s of deactivation, the membrane was depolarized to $+18$ mV again. The channels reactivated from -12 mV and -42 mV with $\tau = 24$ ms and 13 ms, respectively. However, the voltage step from -72 mV back to $+18$ mV reactivated not only the putative M-type K^+ channels, but also other types of channels in the same patch (Fig. 5*C*). Compared with the classical M-current (deactivation $\tau = 103-150$ ms, at approximately -40 mV; Adams *et al.* 1982; Wang *et al.* 1998), our putative M-type channels deactivated with similarly slow kinetics ($\tau = 100 \pm 6$ ms, $n = 3$, at approximately -40 mV). On the other hand, the activation time constant of the putative M-type channels was significantly faster than an estimate of 50 ms for hippocampal M-current (Storm, 1989). Due to the usual presence of other types of K^+ channels in our recordings (and in other native cells as well; Wang *et al.* 1998), a more reliable measurement of M-channel activation was not possible.

Another feature of the macroscopic M-type K^+ current is its sensitivity to muscarinic agonists. In fact, it was the inhibition of this current by muscarinic agonists that led to its name (Brown & Adams, 1980; Storm, 1990). Muscarinic inhibition of M-current involves a second messenger-mediated mechanism. To test whether our M-type K^+ channels were also inhibited by a muscarinic agonist, cell-attached recordings of these channels were performed while 10 μM carbachol was applied in the bath. The channels were first identified by their non-inactivating nature during prolonged membrane depolarization. Channel activities were only analysed from stretches of current traces between 10 and 20 s after the start of the voltage step (Fig. 6*A*), to make sure other types of voltage-dependent K^+ channels were inactivated. Bath application of 10 μM carbachol significantly inhibited channel activities of the M-type K^+ channels (41%, $P < 0.05$, $n = 3$), presumably by activating muscarinic receptors to initiate relevant signalling pathways (Fig. 6). This muscarinic inhibition, together with the real non-inactivating and slow-deactivating nature of this channel, lent strong support to the conclusion that this channel underlies the M-type K^+ current. It should be pointed out, however, that some early studies also identified a muscarine-inhibited component of voltage-independent leak current (Madison *et al.* 1987). It has also been proposed that the M-type and the leak-type K^+ currents may arise from the same channels operating under different conditions (Selyanko & Sim, 1998). Because the putative M-type K^+ channels we recorded were voltage dependent, we felt justified

in categorizing them as M-type rather than leak-type channels.

Delayed-rectifier K^+ channels are the major contributors of sustained K^+ currents in the dendrites

Both the delayed-rectifier and the M-type K^+ channels may contribute to the sustained component of the macroscopic K^+ current, which does not inactivate for several hundred milliseconds (Hoffman *et al.* 1997; Fig. 1). However, compared to the delayed-rectifier K^+ channels, the chances of recording the M-type K^+ channels from the soma or dendrites were very low. In 148 recordings where appropriate voltage protocols were applied to reveal the M-type K^+ channels, these channels were only recorded on 16 occasions (12 somatic recordings, 4 dendritic recordings 170–250 μm from soma). In 15 out of these

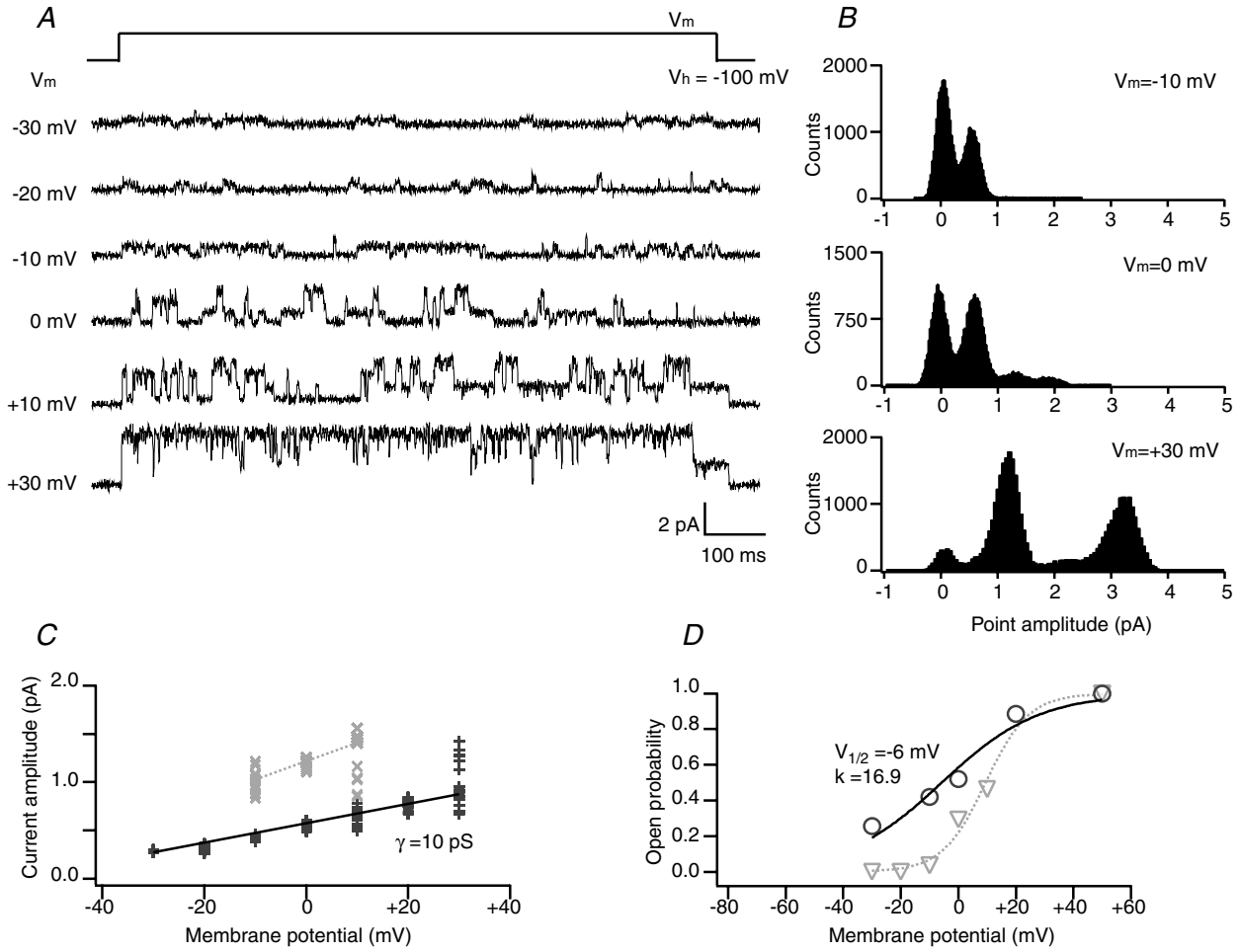

Figure 3. Recording of two different types of K^+ channels in the same patch, 230 μm from soma
A, example traces of channel activities recorded with 0 Ca^{2+} in the recording pipette. Step commands of noted potentials (from a holding potential of −100 mV) were given to the patch. A delayed-rectifier K^+ channel started to open at −20 mV, while the activities of a smaller conductance channel (M-type K^+ channel) could be seen at −30 mV. Activities of both channels increased with depolarization. *B*, current amplitude histograms at noted potentials. At a membrane potential of −10 mV, the histogram has two distinct peaks. The left peak represents current level when both channels were closed, while the right peak represents current level when only the smaller channel alone was open. At this membrane potential, opening of the delayed-rectifier-type channel did not contribute a distinctive current peak to the histogram. At more depolarized potentials, the amplitude histograms have four peaks, representing current levels when both channels were closed, when the smaller channel alone was open, when the delayed-rectifier channel alone was open, and when both channels were open at the same time. *C*, amplitude scatter can be fitted with two lines each representing a conductance level. The delayed-rectifier channel in this recording (grey symbols) had a single-channel conductance (γ) of 19 pS. The M-type K^+ channel had a γ of 10 pS. *D*, open probability of each channel was plotted against membrane potential. Activation of the delayed-rectifier channel was fitted with a single Boltzmann equation which gave $V_{1/2} = +9$ mV and $k = 7.5$ (grey symbols). Activation of the M-type K^+ channel was fitted with a single Boltzmann equation with $V_{1/2} = -6$ mV and $k = 16.9$.

16 occasions, the M-type K^+ channels were recorded together with other types of K^+ channels in the same patch (Figs 3 and 5). Therefore, the density of M-type K^+ channels in both the soma and apical dendrites of CA1 pyramidal neurones seems to be extremely low. On the other hand, the delayed-rectifier K^+ channels were encountered in most cell-attached recordings from the soma and apical dendrites (50–330 μm from soma). The sustained component of the macroscopic K^+ current has a uniform distribution along the dendrites with an average of 8–9 pA per patch when maximally activated (Hoffman *et al.* 1997). We think this component mostly comes from the activities of the delayed-rectifier type K^+ channels. When maximally activated at around +54 mV, single delayed-rectifier K^+ channels generate current amplitudes of approximately 2 pA. Therefore, approximately four such channels per patch would make up an average of 8–9 pA per patch of sustained K^+ currents which are uniformly distributed along the apical dendrites (Hoffman *et al.* 1997).

Slowly inactivating D-type K^+ channels

Besides the rapidly inactivating transient component and the sustained component, a slowly inactivating component was sometimes also present in the macroscopic K^+ currents (Fig. 1).

In four recordings of macroscopic K^+ currents (2 somatic recordings, 2 dendritic recordings 170 and 240 μm from soma), there seemed to be no rapidly inactivating component, but only a slowly inactivating component ($\tau = 98 \pm 5$ ms at approximately +54 mV, $n = 4$) and a non-inactivating (for 400 ms) component. We could separate these two components by a voltage protocol shown in Fig. 7. The recording was at 170 μm from the soma. At the end of a 400 ms depolarizing voltage step (from −97 mV to +53 mV), the membrane was briefly (for 5 ms) hyperpolarized (to −97 mV) before it was depolarized again. The hyperpolarization was brief so that the inactivated channels would not recover and only the non-inactivated channels during the first depolarization remained activated during the second depolarization (Fig. 7). Subtracting the non-inactivating component from the total current resulted in a slowly inactivating ($\tau = 105$ ms) current, which very likely reflected the activities of another population of channels with time-dependent inactivation kinetics different from that of the delayed-rectifier or M-type K^+ channels. Further biophysical analysis of this slowly inactivating component was confounded by the fact that the non-inactivating and rapidly inactivating components were more consistently present and dominated the current in the macroscopic patches.

Single, slowly inactivating K^+ channels, however, were recorded on one occasion (Fig. 8). In this recording at 240 μm from the soma, it appeared that three channels of the same conductance were present, giving rise to four equally spaced peaks in the point amplitude histograms (Fig. 8*B*). These peaks (counting from left to right) corresponded to current levels when none of the channels were open, only one channel was open, two channels were open at the same time, and three channels were open at the same time. Consistent with the notion that these current levels resulted from the activities of three individual channels, the relative proportion of the peaks roughly followed probability relations,

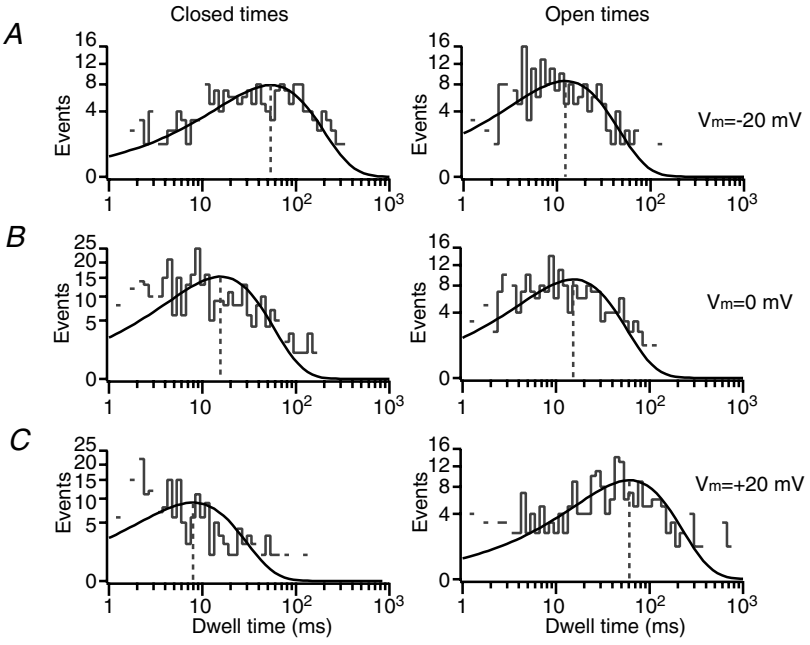

Figure 4. Duration analysis of an M-type channel
Analysis was performed on the M-type channel in Fig. 3. Both closed and open time histograms can be best fitted with single-component exponential distribution functions (continuous lines). Dotted lines mark the time constants of each fit (τ_c and τ_o). *A*, at $V_m = -20$ mV, $\tau_c = 54$ ms, $\tau_o = 12$ ms. *B*, at 0 mV, $\tau_c = 16$ ms, $\tau_o = 15$ ms. *C*, at $V_m = +20$ mV, $\tau_c = 8$ ms, $\tau_o = 61$ ms.

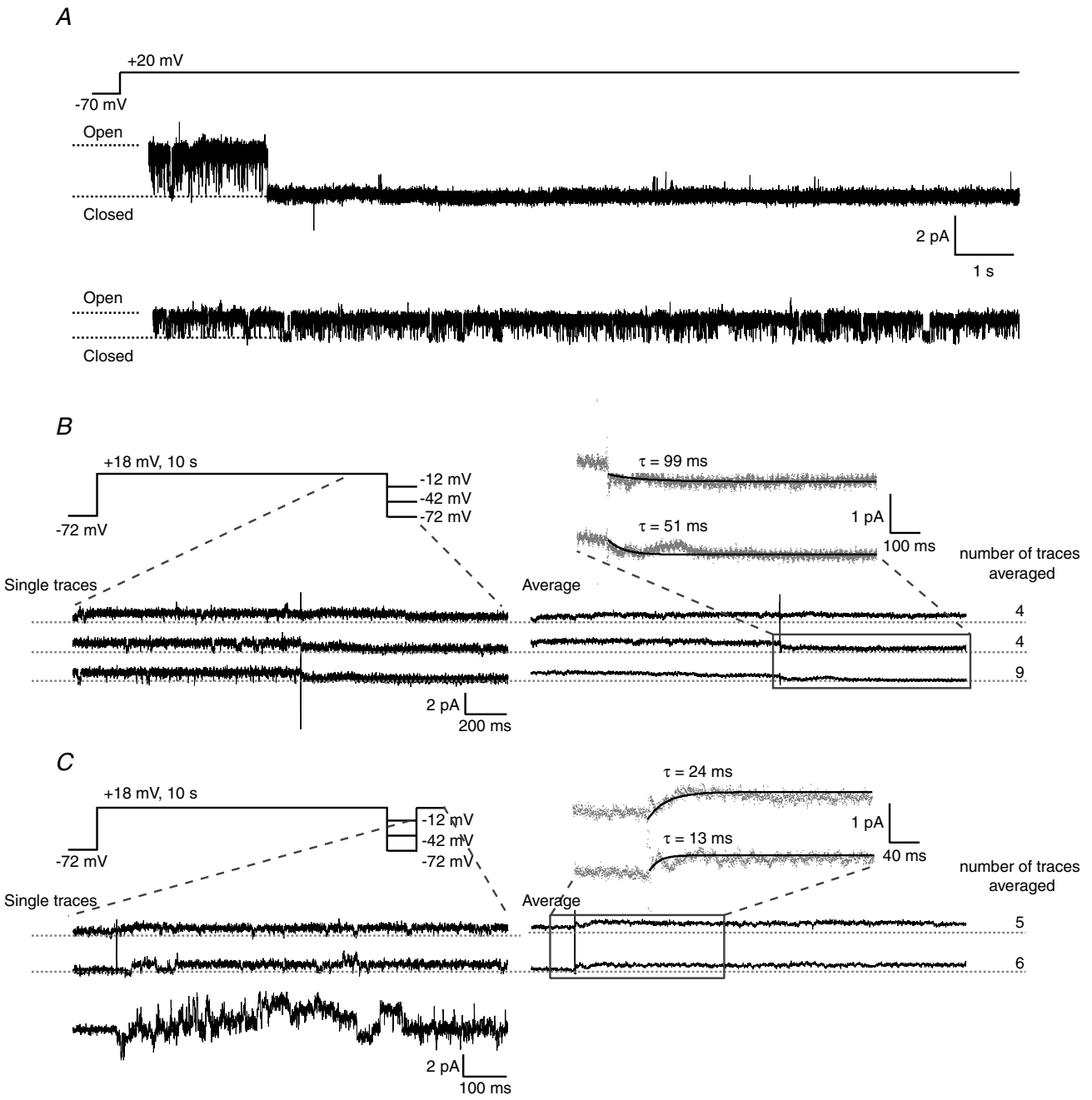

Figure 5. Time-dependent kinetics of the M-type K^+ channels
A, the delayed-rectifier K^+ channel and the M-type K^+ channel have different inactivation properties. In response to a 15 s continuous voltage step to +20 mV (from a holding potential of −70 mV), the delayed-rectifier channel (upper trace, 210 μm from soma) inactivated within 3 s of the start of the step. The M-type channel (lower trace, 230 μm from soma, different patch) did not inactivate for 15 s with depolarization. *B* and *C*, deactivation and reactivation kinetics of the M-type K^+ channel. Recordings were performed from a somatic patch with multiple K^+ channels. The membrane was first depolarized to +18 mV (from −72 mV) for 10 s so that only the M-type K^+ channel remained active. At the end of this 10 s depolarization, the membrane was hyperpolarized to −12, −42 or −72 mV for 1 s to deactivate the channel, after which the membrane was depolarized to +18 mV to reactivate the channel. Example single traces are shown on the left, averages are shown on the right. Dotted lines indicate the current level when the channel was closed. *B*, the M-type K^+ channel deactivated with $\tau = 99$ and 51 ms at −42 and −72 mV, respectively. Channel deactivation was not obvious at −12 mV as there were still appreciable channel activities at this voltage. *C*, from −12 mV, the partially deactivated M-type K^+ channel reactivated with $\tau = 24$ ms as the membrane was depolarized to +18 mV. From −42 mV, the deactivated channel reactivated with $\tau = 13$ ms. From −72 mV, the step to +18 mV reactivated an obvious mixture of different types of K^+ channels.

assuming the presence of three identical channels with similar open probability (Fig. 8*B*). The amplitude scatter graph was also best fitted with three lines (Fig. 8*C*), the slopes of which represent conductance levels when only one of the three channels was open ($\gamma = 19$ pS), when two of the channels were open at the same time ($2\gamma = 37$ pS), and when the three channels were open simultaneously ($3\gamma = 50$ pS). Ensemble averaged current showed complete inactivation at the end of 400 ms voltage steps, with $\tau = 95$ ms at +54 mV (Fig. 8*A*), which matches well with the time-dependent inactivation kinetics of the slowly inactivating component in the macroscopic current (Figs 1 and 7). Such time-dependent inactivation was faster than the inactivation of the delayed rectifier K^+ channels (see above), yet slower than that of the A-type K^+ channels (see below), which makes this type of channel best suited to account for the D-type K^+ current (Storm, 1988). Both single-channel conductance ($\gamma = (19 + 37/2 + 50/3)/3 = 18$ pS) and voltage-dependent activation ($V_{½} = +4$ mV, $k = 6$) of this type of channel were similar to those of the delayed-rectifier K^+ channel. The D-type K^+ channels, however, did inactivate in a voltage-dependent manner, with $V_{½} = -20$ mV for half-maximum inactivation, and a slope factor of $k = 8$ (Fig. 8*D*).

Fast inactivating A-type K^+ channels

Single, fast inactivating A-type K^+ channels were recorded from somatic ($n = 1$) and dendritc patches ($n = 5$) of up to 215 μm from the soma. Recordings from more distal parts of the dendrites often resulted in prominent macroscopic A-type K^+ currents, while single channels were rarely encountered. The A-type K^+ channels we recorded had fairly small single-channel conductances (Fig. 9*A* and *B*) ($\gamma = 6 \pm 0.6$ pS, $n = 3$), and could be easily distinguished from other types of voltage-dependent K^+ channels by their rapid time-dependent inactivation ($\tau = 23 \pm 2$ ms, $n = 5$) (Fig. 9*A*). Voltage-dependent activation of the A-type K^+ channels reached half-maximum activation at

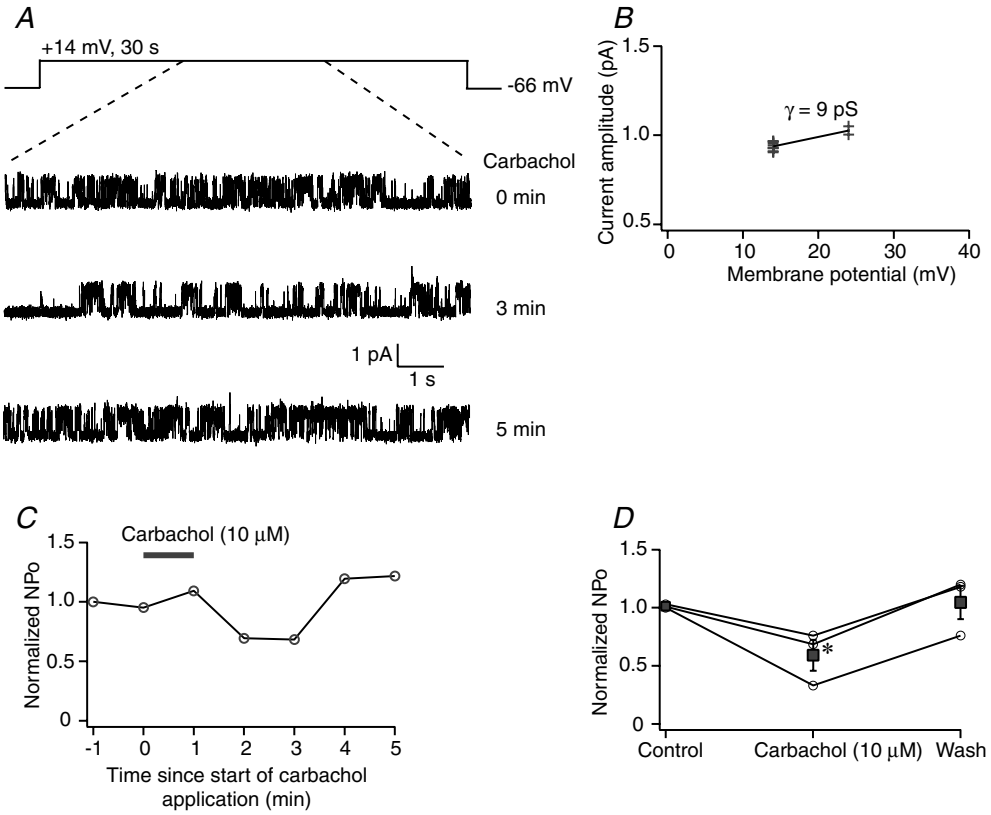

Figure 6. Carbachol (10 μM) inhibited the activity of the M-type K^+ channels
A, one example recording from the soma. The membrane was held at −66 mV and depolarized to +14 mV for 30 s. Channel activities between 10 and 20 s after the start of the voltage step were analysed. Bath application of 10 μM carbachol reduced channel activity. *B*, conductance of this channel was estimated to be 9 pS, which is within the range for M-type K^+ channels. *C*, carbachol was perfused for 1 min in the bath. Channel activities were inhibited, and the effect could be washed off. *D*, similar experiments were performed in three recordings, all of which were from the soma. Carbachol inhibited channel activities of the M-type K^+ channels in all three cases, with a mean of 41% inhibition as compared to control ($P < 0.05$).

$V_{1/2} = +5$ mV (Fig. 9*C*, fitting of mean normalized peak conductance from 5 recordings), which was similar to half-maximum activation voltages for the delayed-rectifier and D-type K^+ channels. However, the voltage-dependent activation of the A-type K^+ channels had a much slower slope ($k = 16$), and thus a wider voltage range for activation (Table 2). Voltage-dependent inactivation of the A-type K^+ channels could also be fitted with a single Boltzmann equation with $V_{1/2} = -64$ mV and $k = 9$ (Fig. 9*C*, mean normalized peak current from 3 recordings).

Discussion

Cell-attached recordings reveal the diversity of K^+ channels in the dendrites of CA1 pyramidal neurones

With cell-attached recordings of macroscopic K^+ currents and single K^+ channels, our study provided direct biophysical evidence for the presence of multiple types of voltage-dependent K^+ channels not only in the soma, but also in the apical dendrites of CA1 pyramidal neurones (Fig. 10). We focused on the biophysical properties of the channels, because both time- and voltage-dependent properties of K^+ channels are important in determining how electrical signals are propagated.

Compared with other recording configurations (whole-cell or outside-out recordings), voltage-clamp recording in the cell-attached configuration became our method of choice, because with cell-attached recordings adequate voltage control could be achieved while preserving intracellular components that may be important for channel properties. We categorized our K^+ channels into delayed-rectifier, M-type, D-type and A-type, mostly based on their differences in time-dependent inactivation kinetics. Detailed analyses of channel biophysics were performed only when a certain channel type could be unambiguously identified or isolated, mostly with recordings where single channels could be resolved.

The first indication of the presence of multiple types of K^+ channels was the large variability in the waveforms of macroscopic K^+ currents at similar locations along the dendrites (Fig. 1). Such variability probably reflected the fact that each cell-attached recording sampled a distinct combination of K^+ channels with different time-dependent inactivation kinetics, and that some of these channels may be more or less clustered on the dendritic membrane. On the other hand, such variability made it quite implausible to include channel blockers in the cell-attached electrode and compare the amplitude and/or waveform of macroscopic currents between patches. Nonetheless, pharmacology could be used to help identify channel types if the pharmacological agents either act through a non-membrane-delimited, second messenger-mediated mechanism, or are membrane permeable and act on the inside of the channel. We therefore also used the muscarinic agonist carbachol to help identify the M-type K^+ channels.

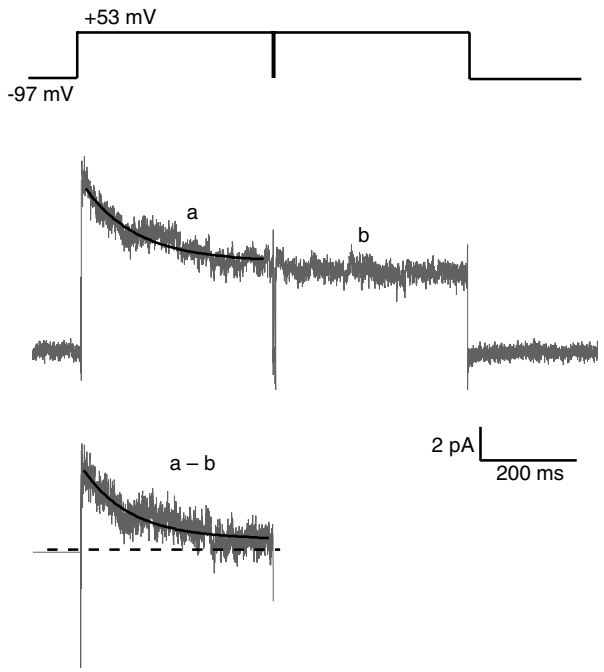

Figure 7. A slowly inactivating component of macroscopic K^+ currents
The recording was made 170 μm from the soma, in which a double-pulse protocol was used to separate the slowly inactivating component from the non-inactivating component of the macroscopic K^+ current. In the voltage protocol, two steps to +53 mV (from a holding potential of −97 mV, each lasting 400 ms) were separated by a 5 ms hyperpolarization to −97 mV. Current trace was an average of 5 sweeps. Subtracting the non-inactivating component (b) from the total current (a) resulted in isolation of a slowly inactivating component with $\tau = 105$ ms. ($\tau = 110$ ms with an exponential fitting of the total current (a) before subtraction.)

Comparison to single-channel data in other experimental systems

The A-type K^+ channels we recorded from the dendrites of CA1 pyramidal neurones had a smaller single-channel conductance (6 pS) than that of the A-type K^+ channels recorded from the dendrites of layer V pyramidal neurones in neocortex (13 pS) (Korngreen & Sakmann, 2000). A similar difference in single-channel conductance was first demonstrated between the *Shaker* and the *Shal* K^+ channels in *Drosophila*. Although both encoding A-type K^+ currents, the *Shaker* channels have a conductance of 12–16 pS while the single-channel conductance of the *Shal* channels is 5–9 pS (Solc *et al.* 1987). Our dendritic A-type K^+ channels therefore resembled the *Shal* channels more than the *Shaker* channels – an observation that lends further support to

the notion that members of the Kv4 family of K^+ channels are the major contributors of dendritic A-type K^+ current in hippocampal CA1 pyramidal neurones (Sheng *et al.* 1992). Furthermore, mammalian Kv4 genes form channels of similar conductance (5–6 pS; Baldwin *et al.* 1991; Jerng *et al.* 1999; Holmqvist *et al.* 2002) to our A-type K^+ channels when expressed in *Xenopus* oocytes. The channel opening events of our A-type K^+ channels were not square-shaped like the delayed-rectifier, D-type, or M-type K^+ channels, but instead had a 'serrated' appearance that is typical of single mammalian Kv4 channels (Fig. 9) (Baldwin *et al.* 1991; Jerng *et al.* 1999; Holmqvist *et al.* 2002). On the other hand, the time- and voltage-dependent kinetic properties of expressed Kv4 channels are different from those of our A-type K^+ channels (Baldwin *et al.* 1991; Jerng *et al.* 1999; Holmqvist *et al.* 2002). The disparity is likely to result from differences in preparation, state of phosphorylation, and/or the temperature at which measurements were taken.

Our D-type K^+ channels, on the other hand, had a larger single-channel conductance (18 pS) that is reminiscent of the slowly inactivating K^+ channels recorded in PC12 cells (20 pS), which are most likely encoded by members of the Kv1 family of K^+ channel genes such as Kv1.2 (Conforti & Millhorn, 1997). Both the single-channel

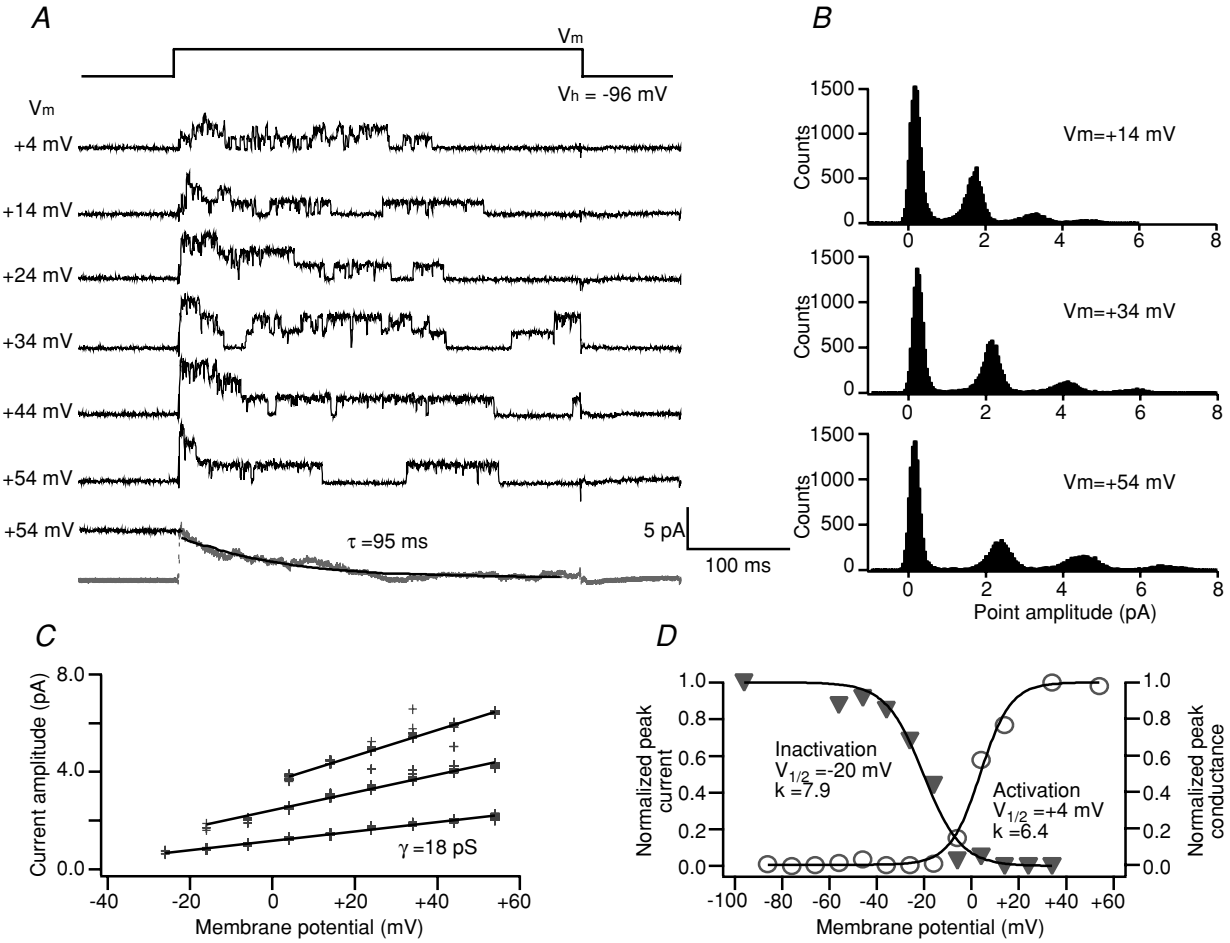

Figure 8. Single D-type K^+ channels recorded 240 μm from soma
A, three identical channels were present in this recording. The patch membrane was held at −96 mV. 400 ms depolarizing steps of noted potentials activated three K^+ channels in a voltage-dependent manner. Bottom trace is the ensemble average of channel activities at +54 mV (average of 9 traces). At this potential, current inactivated with a time constant (τ) of 95 ms. *B*, amplitude histograms of this recording have four peaks, representing current levels when none of the channels was open, when only one channel was open, when two channels were open at the same time, and when three channels were open at the same time. Distances between the peaks were nearly identical, indicating that the channels were of similar conductance. *C*, amplitude scatter could be fitted with three lines with slope values of 19 pS (γ), 37 pS (2γ) and 50 pS (3γ), respectively. *D*, activation and inactivation curves were constructed using peak conductance and peak current values measured from ensemble averages at noted membrane potentials. Activation and inactivation are both fitted with single Boltzmann equations. For activation, $V_{1/2} = +4$ mV, $k = 6.4$. For inactivation, $V_{1/2} = -20$ mV, $k = 7.9$.

conductance and the slowly inactivating kinetics of the D-type channels also bear a striking resemblance to the K_{AT} channels of CA3 neurones in organotypic slice culture (19 pS, with inactivation time constant of 20–100 ms; Bossu & Gahwiler, 1996). It was proposed that the K_{AT} channel, as one single molecular entity, can undergo different gating modes and give rise to either a non-inactivating ensemble current or an inactivating ensemble current, and switch between different gating modes even during the same recording (Bossu & Gahwiler, 1996). The single-channel conductance of our D-type channels (18 pS) was very similar to our delayed-rectifier channels (19 pS). But the channels we recorded did not seem to switch gating modes (from inactivating to non-inactivating or vice versa) during the same recording. For this reason, we tend to favour the conclusion that the D-type and the delayed-rectifier channels were of separate molecular entities. However, we did have a small number of recordings of isolated D-type channels. Therefore we cannot completely exclude the possibility that these two types of channel behaviours could have come from the same channels locked in different gating modes.

In cultured hippocampal neurones, it has been demonstrated that the Kv2.1 K^+ channels are the major contributors of delayed-rectifier K^+ currents (Murakoshi & Trimmer, 1999), and that Kv2.1 protein is preferentially located in soma and proximal dendrites of pyramidal neurones (Lim *et al.* 2000). It is therefore possible that delayed-rectifier K^+ channels in distal dendrites may have different molecular composition from those in the soma and proximal dendrites. We recorded one type of delayed-rectifier K^+ channel from somatic and dendritic patches of up to 300 μm from soma. We did not observe any dramatic difference in single-channel properties between delayed-rectifier channels in the soma, proximal dendrites, or distal dendrites. Any change introduced by their possibly different molecular compositions may therefore be quite subtle. Nevertheless, the single-channel conductance of our delayed-rectifier K^+ channels (19 pS) did match well with the single-channel conductance of expressed mammalian Kv2.1 channels (17 pS) (Patton *et al.* 1997) or Kv2.2 channels (15 pS) (Schmalz *et al.* 1998). This conductance is also similar to the single-channel conductance of delayed-rectifier K^+ channels (15–20 pS) recorded in culture (Rogawski, 1986), the K_{AT} channels (19 pS) in cultured slices (Bossu & Gahwiler, 1996), and one of the sustained K^+ channels (16 pS) up-regulated by arachidonic acid in CA1 pyramidal neurones (Colbert & Pan, 1999). Each of these previously described channels gives rise to a non-inactivating ensemble current of several hundred milliseconds.

Single, non-inactivating M-/leak-type K^+ channels have been previously recorded in cultured hippocampal

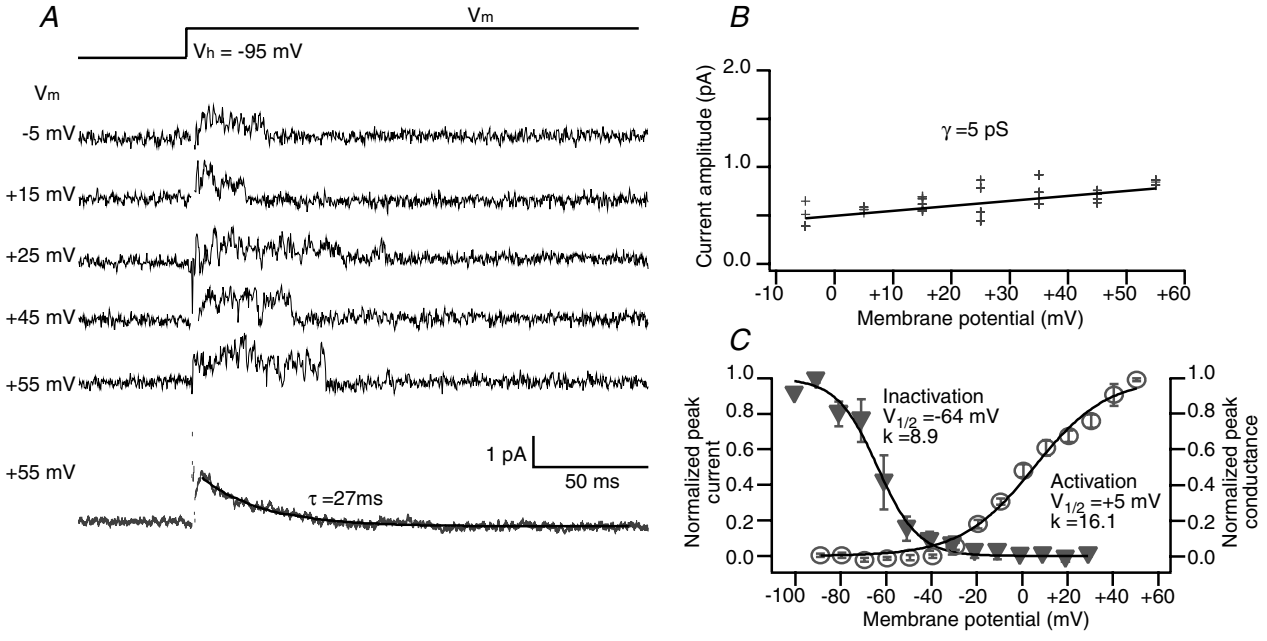

Figure 9. Single dendritic A-type K^+ channel
A, single, fast inactivating A-type K^+ channel recorded 120 μm from soma. The patch was held at −95 mV, and voltage steps of noted potentials were given to activate the channel. Bottom trace is ensemble average at +55 mV (average of 28 traces). Current inactivated with $\tau = 27$ ms in this particular recording. *B*, current amplitude scatter graph was fitted with a line that gave a single-channel conductance of 5 pS for this channel. *C*, activation ($n = 6$) and inactivation ($n = 3$) curves were constructed using peak conductance and peak current values measured from ensemble averages at noted membrane potentials. Activation and inactivation were both fitted with single Boltzmann equations. For activation, $V_{1/2} = +5$ mV, $k = 16.1$. For inactivation, $V_{1/2} = -64$ mV, $k = 8.9$.

neurones (Selyanko & Sim, 1998). Those are truly non-inactivating just like the M-type K^+ channels we identified in our recordings but with smaller single-channel conductance (7 pS as compared to 11 pS in our recordings). Also, those channels reported by Selyanko & Sim were inhibited by external Ca^{2+}. We recorded M-type K^+ channels with either 2 mM Ca^{2+} (2 out of 16 recordings) or 0 Ca^{2+} (14 out of 16 recordings) in the recording pipettes, and always 2 mM Ca^{2+} in external solution. Like the Ca^{2+}-inhibited K^+ channels in culture, our M-type K^+ channels were inhibited by muscarinic agonists that acted through a second messenger-mediated mechanism.

It is important to point out that comparisons of single-channel properties between different preparations should be taken with great caution, because differences in recording conditions – such as ion composition of the solutions and recording configurations – can affect the results. Given the diversity of K^+ channel genes, as well as further complication introduced by possible heteromultimerization and addition of auxiliary subunits, attempts to definitively match native currents with cloned genes are far from trivial. In light of these considerations, the comparison and correlations discussed above are obviously more suggestive than conclusive. Nevertheless, our description of single-channel properties provides groundwork for future studies that aim at determining molecular substrates for the various types of K^+ channels in CA1 pyramidal neurone dendrites.

Distribution of K^+ channels along the apical dendrite of CA1 pyramidal neurones

In previous studies of dendritic, macroscopic K^+ currents, a distinction was made between a rapidly inactivating transient component (i.e. the A-type K^+ current) and a non-inactivating (for several hundred milliseconds) sustained component. The mean density of A-type K^+ channels increases up to fivefold from the soma to the very tip of the apical dendrite, whereas the sustained component has uniform distribution (Hoffman *et al.* 1997). The amplitude of macroscopic A-type K^+ currents varies from patch to patch (Hoffman *et al.* 1997; Fig. 1), suggesting a 'clustered' fashion of channel distribution. An increase in mean channel density along the dendrites may therefore result from an increased probability of encountering large clusters of A-type K^+ channels in distal dendrites.

Both the delayed-rectifier and the M-type K^+ channels are non-inactivating for several hundred milliseconds, and therefore could contribute to the sustained component of macroscopic K^+ current previously described (Hoffman *et al.* 1997). However, the chances of encountering the M-type K^+ channels were extremely low, so that the delayed-rectifier K^+ channels are very likely the major contributors to the sustained K^+ current.

Although the low probability of encountering the M-type K^+ channels led us to conclude that these channels were of extremely low density in the soma/apical dendrite region of CA1 pyramidal neurones, it is also possible that these channels were inhibited under our experimental conditions, and some manipulations are needed to make the channels 'appear' in the recordings. We eliminated Ca^{2+} from our pipette solution, but this did not increase our chances of encountering these channels. Effects of other channel agonists will need to be studied in the future.

In cultured hippocampal neurones, Kv2.1 proteins form clusters in the soma and proximal dendrites while Kv2.2 proteins are uniformly distributed in the soma and along the dendrites (Lim *et al.* 2000; Antonucci *et al.* 2001). Our delayed-rectifier channels are uniformly distributed along the dendrites, which is consistent with previous studies (Hoffman *et al.* 1997). We have not recorded, even from the soma, the dramatically large sustained current that would be expected for big Kv2.1 protein clusters in cultured neurones. We think that the differences in the preparation and age of the animals may contribute to this discrepancy.

The presence of the D-type K^+ channels was reflected from the occasional presence of a slowly inactivating component in the macroscopic current (Figs 1 and 7). Single D-type K^+ channels were only resolved on one occasion, with three identical channels coexisting in the same patch (Fig. 8). Very little can be said about the distribution of D-type K^+ channels. Our guess is that they are in the dendrites, but with a lower density than the delayed-rectifier-type K^+ channels. In both the hippocampal CA1 pyramidal neurones (Hoffman *et al.*

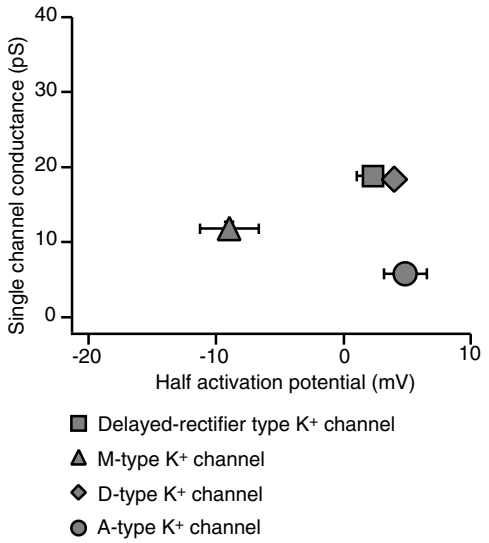

Figure 10. Summary of multiple types of dendritic K^+ channels
Four types of voltage-dependent K^+ channels were identified with single-channel analysis.

1997; Golding *et al.* 1999) and the layer V pyramidal neurones of neocortex (Bekkers & Delaney, 2001), it was demonstrated that a 4-aminopyridine- and/or dendrotoxin-sensitive current only contributes to a small fraction (∼20% in CA1 neurones and < 6% in layer V neurones) of K^+ currents recorded in the outside-out configuration. This is consistent with the D-type channels having a low-density distribution in the dendrites.

Functional implications

In early studies of dendritic K^+ current, great success was achieved by separating the macroscopic current into a transient component and a sustained component. The transient component, because of its rapid inactivation and prominent dendritic presence, was easily distinguished from other current components. Studies of this transient current (the A-type K^+ current) provided the best example to date of a prominent dendritic current that underlies many aspects of dendritic function and plasticity (Hoffman *et al.* 1997; Hoffman & Johnston, 1998; Watanabe *et al.* 2002; Yuan *et al.* 2002; Frick *et al.* 2004).

On the other hand, some aspects of dendritic signalling remain to be explained. For example, with a high density of A-type K^+ current, why is the repolarization of back-propagating action potentials slower in the dendrites than in the soma? With a uniform distribution of Na^+ channels (Magee & Johnston, 1995), why is the initial dV/dt of back-propagating action potentials smaller in the dendrites than in the soma? To answer these questions, studies of other types of K^+ channels may provide some clues.

The approach we took was to record single K^+ channels from the dendrites, and describe their biophysical properties with enough detail and precision so as to categorize them into different types. Besides the A-type K^+ channels, the apical dendrites of CA1 pyramidal neurones also express delayed-rectifier, D-type and M-type K^+ channels. Depending on their biophysical properties and modulation, these channels could also contribute to various aspects of dendritic function. The D-type K^+ channels, for example, were proposed to contribute to setting the threshold for Ca^{2+} spikes in CA1 pyramidal neurones, so that the lack of D-type K^+ channels would make it easier to initiate Ca^{2+} spikes in the dendrites (Golding *et al.* 1999). The functions of delayed-rectifier and M-type K^+ channels in the dendrites have not been extensively studied, and remain to be explored in the future.

References

Adams PR, Brown DA & Constanti A (1982). M-currents and other potassium currents in bullfrog sympathetic neurones. *J Physiol* **330**, 537–572.

Antonucci DE, Lim ST, Vassanelli S & Trimmer JS (2001). Dynamic localization and clustering of dendritic Kv2.1 voltage-dependent potassium channels in developing hippocampal neurons. *Neuroscience* **108**, 69–81.

Baldwin TJ, Tsaur ML, Lopez GA, Jan YN & Jan LY (1991). Characterization of a mammalian cDNA for an inactivating voltage-sensitive K^+ channel. *Neuron* **7**, 471–483.

Bekkers JM & Delaney AJ (2001). Modulation of excitability by alpha-dendrotoxin-sensitive potassium channels in neocortical pyramidal neurons. *J Neurosci* **21**, 6553–6560.

Bossu JL & Gahwiler BH (1996). Distinct modes of channel gating underlie inactivation of somatic K^+ current in rat hippocampal pyramidal cells in vitro. *J Physiol* **495**, 383–397.

Brown DA & Adams PR (1980). Muscarinic suppression of a novel voltage-sensitive K^+ current in a vertebrate neurone. *Nature* **283**, 673–676.

Colbert CM & Pan E (1999). Arachidonic acid reciprocally alters the availability of transient and sustained dendritic K^+ channels in hippocampal CA1 pyramidal neurons. *J Neurosci* **19**, 8163–8171.

Colquhoun D & Sigworth FJ (1995). Fitting and statistical analysis of single-channel records. In *Single-Channel Recording*, 2nd edn, ed. Sakmann B & Neher E, pp. 483–587. Plenum Press, New York and London.

Conforti L & Millhorn DE (1997). Selective inhibition of a slow-inactivating voltage-dependent K^+ channel in rat PC12 cells by hypoxia. *J Physiol* **502**, 293–305.

Frick A, Magee J & Johnston D (2004). LTP is accompanied by an enhanced local excitability of pyramidal neuron dendrites. *Nat Neurosci* **7**, 126–135.

Fricker D, Verheugen JA & Miles R (1999). Cell-attached measurements of the firing threshold of rat hippocampal neurones. *J Physiol* **517**, 791–804.

Golding NL, Jung HY, Mickus T & Spruston N (1999). Dendritic calcium spike initiation and repolarization are controlled by distinct potassium channel subtypes in CA1 pyramidal neurons. *J Neurosci* **19**, 8789–8798.

Hausser M, Spruston N & Stuart GJ (2000). Diversity and dynamics of dendritic signaling. *Science* **290**, 739–744.

Hoffman DA & Johnston D (1998). Downregulation of transient K^+ channels in dendrites of hippocampal CA1 pyramidal neurons by activation of PKA and PKC. *J Neurosci* **18**, 3521–3528.

Hoffman DA, Magee JC, Colbert CM & Johnston D (1997). K^+ channel regulation of signal propagation in dendrites of hippocampal pyramidal neurons. *Nature* **387**, 869–875.

Holmqvist MH, Cao J, Hernandez-Pineda R, Jacobson MD, Carroll KI, Sung MA, Betty M, Ge P, Gilbride KJ, Brown ME, Jurman ME, Lawson D, Silos-Santiago I, Xie Y, Covarrubias M, Rhodes KJ, Distefano PS & An WF (2002). Elimination of fast inactivation in Kv4 A-type potassium channels by an auxiliary subunit domain. *Proc Natl Acad Sci U S A* **99**, 1035–1040.

Jerng HH, Shahidullah M & Covarrubias M (1999). Inactivation gating of Kv4 potassium channels: molecular interactions involving the inner vestibule of the pore. *J General Physiol* **113**, 641–660.

Johnston D, Magee JC, Colbert CM & Christie BR (1996). Active properties of neuronal dendrites. *Annu Rev Neurosci* **19**, 165–186.

Korngreen A & Sakmann B (2000). Voltage-gated K^+ channels in layer 5 neocortical pyramidal neurones from young rats: subtypes and gradients. *J Physiol* **525**, 621–639.

Lim ST, Antonucci DE, Scannevin RH & Trimmer JS (2000). A novel targeting signal for proximal clustering of the Kv2.1 K^+ channel in hippocampal neurons. *Neuron* **25**, 385–397.

Madison DV, Lancaster B & Nicoll RA (1987). Voltage clamp analysis of cholinergic action in the hippocampus. *J Neurosci* **7**, 733–741.

Magee JC (1998). Dendritic hyperpolarization-activated currents modify the integrative properties of hippocampal CA1 pyramidal neurons. *J Neurosci* **18**, 7613–7624.

Magee JC & Johnston D (1995). Characterization of single voltage-gated Na^+ and Ca^{2+} channels in apical dendrites of rat CA1 pyramidal neurons. *J Physiol* **487**, 67–90.

Megias M, Emri Z, Freund TF & Gulyas AI (2001). Total number and distribution of inhibitory and excitatory synapses on hippocampal CA1 pyramidal cells. *Neuroscience* **102**, 527–540.

Mickus T, Jung HY & Spruston N (1999). Properties of slow, cumulative sodium channel inactivation in rat hippocampal CA1 pyramidal neurons. *Biophys J* **76**, 846–860.

Mitterdorfer J & Bean BP (2002). Potassium currents during the action potential of hippocampal CA3 neurons. *J Neurosci* **22**, 10106–10115.

Murakoshi H & Trimmer JS (1999). Identification of the Kv2.1 K^+ channel as a major component of the delayed rectifier K^+ current in rat hippocampal neurons. *J Neurosci* **19**, 1728–1735.

Patton DE, Silva T & Bezanilla F (1997). RNA editing generates a diverse array of transcripts encoding squid Kv2 K^+ channels with altered functional properties. *Neuron* **19**, 711–722.

Rogawski MA (1986). Single voltage-dependent potassium channels in cultured rat hippocampal neurons. *J Neurophysiol* **56**, 481–493.

Schmalz F, Kinsella J, Koh SD, Vogalis F, Schneider A, Flynn ER, Kenyon JL & Horowitz B (1998). Molecular identification of a component of delayed rectifier current in gastrointestinal smooth muscles. *Am J Physiol* **274**, G901–G911.

Selyanko AA & Sim JA (1998). Ca^{2+}-inhibited non-inactivating K^+ channels in cultured rat hippocampal pyramidal neurones. *J Physiol* **510**, 71–91.

Sheng M, Tsaur ML, Jan YN & Jan LY (1992). Subcellular segregation of two A-type K^+ channel proteins in rat central neurons. *Neuron* **9**, 271–284.

Solc CK, Zagotta WN & Aldrich RW (1987). Single-channel and genetic analyses reveal two distinct A-type potassium channels in Drosophila. *Science* **236**, 1094–1098.

Storm JF (1988). Temporal integration by a slowly inactivating K^+ current in hippocampal neurons. *Nature* **336**, 379–381.

Storm JF (1989). An after-hyperpolarization of medium duration in rat hippocampal pyramidal cells. *J Physiol* **409**, 171–190.

Storm JF (1990). Potassium currents in hippocampal pyramidal cells. *Prog Brain Res* **83**, 161–187.

Wang HS, Pan Z, Shi W, Brown BS, Wymore RS, Cohen IS, Dixon JE & McKinnon D (1998). KCNQ2 and KCNQ3 potassium channel subunits: molecular correlates of the M-channel. *Science* **282**, 1890–1893.

Watanabe S, Hoffman DA, Migliore M & Johnston D (2002). Dendritic K^+ channels contribute to spike-timing dependent long-term potentiation in hippocampal pyramidal neurons. *Proc Natl Acad Sci U S A* **99**, 8366–8371.

Yuan LL, Adams JP, Swank M, Sweatt JD & Johnston D (2002). Protein kinase modulation of dendritic K^+ channels in hippocampus involves a mitogen-activated protein kinase pathway. *J Neurosci* **22**, 4860–4868.

Acknowledgements

We would like to thank Dr Rick Gray for expert advice. This research was supported by NIH grants NS37444, MH48432 and MH44754.

Author's present address

D. Johnston: Institute for Neuroscience, Center for Learning and Memory, University of Texas, Austin, TX78712, USA.